JOURNAL OF SPACECRAFT AND ROCKETS
Vol. 30, No. 6, November–December 1993

Rapid Generation of Site/Satellite Timetables

Salvatore Alfano*
Phillips Laboratory, Albuquerque, New Mexico 87117

This paper presents a numerical method to rapidly determine visibility periods of a satellite for a ground station having restrictions in azimuth, elevation, and range. The algorithm uses pairs of fourth-order polynomials (quartic blending) to construct waveforms that represent the restricted parameters vs time for an oblate Earth. These waveforms are produced from either uniform or arbitrarily spaced data points; viewing times are obtained by extracting the real roots of localized quintic polynomials. This algorithm works for all orbital eccentricities and perturbed satellite motion, provided the functions do not become discontinuous. Results from this algorithm are almost identical to those obtained by modeling satellites subject to first-order secular perturbations caused by mass anomalies but generated with an 89% decrease in computation time over a 5-s step brute force method. Advantages of this numerical method include compact storage and ease of calculation, making it attractive for supporting ground-based satellite operations.

Nomenclature

$C(T)$ = quintic polynomial
$C_t(T)$ = quintic polynomial for time
e = eccentricity
e_e = eccentricity of the Earth ellipsoid
$F(\tau)$ = quartic polynomial
$f_{\beta_{LIM}}(t)$ = azimuth limit crossing function
$f_{\phi_{LIM}}(t)$ = elevation limit crossing function
$f_{RANGE}(t)$ = range limit crossing function
H = altitude deviation from the Earth ellipsoid
i = inclination
J_2 = second harmonic coefficient
$\bar{n}$ = anomalistic mean motion
n_0 = mean motion at epoch
P = first quartic polynomial
P_i = ith data point for quartic blending
p = semilatus rectum
p_i = ith data point for quartic polynomial
Q = second quartic polynomial
$R(t)$ = range
R_{LIM} = range limit
$r_{SAT}(t)$ = geocentric IJK satellite position vector
$r_{SITE}(t)$ = geocentric IJK site position vector
T = quintic polynomial argument
T_{ROOT} = real unique root of $C(T)$
t = time
α_i = ith quintic polynomial coefficient
$\beta(t)$ = azimuth angle
β_{LIM} = azimuth limit
γ_i = ith quartic polynomial coefficient
Δt = simulation step size for time
θ = local sidereal angle
$\rho_{IJK}(t)$ = IJK vector from site to satellite
$\rho_E(t)$ = east component of $\rho_{SEZ}(t)$
$\rho_S(t)$ = south component of $\rho_{SEZ}(t)$
$\rho_{SEZ}(t)$ = topocentric SEZ vector from site to satellite
$\rho_Z(t)$ = zenith component of $\rho_{SEZ}(t)$
τ = quartic polynomial argument
$\phi(t)$ = elevation angle
ϕ_{LIM} = elevation limit
ϕ_{LAT} = station geodetic latitude
$\dot{\Omega}$ = nodal rate
$\dot{\omega}$ = periapsis rate

Received July 18, 1992; revision received Nov. 10, 1992; accepted for publication Nov. 11, 1992.

*Chief, Space and Missiles Dynamics Division; mailing address: PL/VTA, 3550 Aberdeen Ave. SE, Kirtland AFB, NM, 87117-5776. Senior Member AIAA.

Introduction

THE traditional timetable generation problem consists of determining the viewing periods of a satellite vs an Earth-fixed tracking station with azimuth, elevation, and range restrictions. With few satellites aloft, the early days of satellite operations consisted of establishing communications whenever a vehicle entered the ground station's visibility window. With a tabulation of viewing times and antenna-pointing parameters, satellite operators were prepared to transmit and receive data from the vehicle. These operations have changed significantly. Satellites are now deployed with mission effectiveness highly reliant on spaceborne tracking and crosslink communications. Manufacturers currently design satellites to be operator interactive even when outside the visibility window of a ground station. Mission designers are concerned with how a satellite deployment strategy *loads* a ground station, as well as the frequency and duration of high conflicts. This is a key orbit-design issue because competition for ground station support is usually resolved with the highest priority satellite awarded support. Also, as the satellite altitude decreases, the opportunities to track or communicate with the vehicle from a ground station become more restricted, further complicating the satellite scheduling process. These issues call for a computationally efficient routine to generate a timetable of visibility periods, capable of processing all orbit types against any ground station.

Site/satellite visibility periods are typically determined by evaluating Earth-centered inertial position vectors of the two objects of interest. An orbital simulation is advanced in time by some small time increment Δt and a visibility check is performed at each step. One drawback to this method is computation time, especially when modeling many perturbations and processing several vehicles. An additional disadvantage can be the imprecision of the satellite viewing determination resulting from the simulation step size Δt. Escobal[1] proposed a faster method to solve the satellite vs Earth-fixed tracking station problem by developing a closed-form solution for the unrestricted visibility periods about an oblate Earth. Escobal transforms the satellite and tracking station geometry into a single transcendental equation as a function of eccentric anomaly; numerical methods are then used to find the rise and set anomalies, if they exist. More recently, Lawton[2] developed a method to find visibility periods for vehicles in circular or near-circular orbits by approximating an unrestricted visibility function with a Fourier series. Exploiting the sinusoidal nature

of the visibility curve generated by satellites with orbital eccentricities less than 0.1, he determines the local periodicity of this curve and then uses a numerical search to locate viewing times. This method works well for low eccentricity orbits but fails for more elliptical orbits because the visibility waveform becomes aperiodic.

The method of ratios[3] has been used to compute average access time and is a good prefilter for identifying satellites that are always out of range or have improper geometry for viewing. Parabolic blending has also been used to determine satellite visibility with range restrictions[4] and can be used as a prefilter. This paper extends that work, presenting a highly accurate, computationally efficient, numerical method to construct a site/satellite timetable for all orbit types given a ground station with azimuth, elevation, and range restrictions.

Azimuth, Elevation, and Range Functions

Let $r_{\mathrm{SITE}}(t)$ be the Earth-centered inertial position vector of the ground station and $r_{\mathrm{SAT}}(t)$ be the corresponding satellite position at time t. Define the vector from the site to the satellite, $\rho_{IJK}(t)$, as

$$\rho_{IJK}(t) = r_{\mathrm{SAT}}(t) - r_{\mathrm{SITE}}(t) \tag{1}$$

This vector is easily transformed to the topocentric coordinate system,[5] becoming $\rho_{SEZ}(t)$. The azimuth $\beta(t)$ is computed as

$$\beta(t) = \tan^{-1}\left[\frac{\rho_E(t)}{-\rho_S(t)}\right] \tag{2}$$

with a check performed to insure $\beta(t)$ is in the proper quadrant. The elevation $\phi(t)$ is defined as

$$\phi(t) = \tan^{-1}\left[\frac{\rho_Z(t)}{\sqrt{\rho_S^2(t) + \rho_E^2(t)}}\right] \tag{3}$$

with the range $R(t)$ being

$$R(t) = \sqrt{\rho_S^2(t) + \rho_E^2(t) + \rho_Z^2(t)} \tag{4}$$

Tabulating the components $\rho_S(t)$, $\rho_E(t)$, and $\rho_Z(t)$ at user-chosen time intervals, the curve fitting is accomplished by approximating waveforms for azimuth, elevation, and range crossings with localized quintic polynomials. (The interval at which the topocentric components are tabulated is designer chosen, but the reader is cautioned against choosing a step too large. As the interval is increased, this most certainly will result in *missed* crossing times for rapidly varying data.) To determine when an azimuth limit β_{LIM} is crossed, define the function

$$f_{\beta_{\mathrm{LIM}}}(t) = \rho_E(t) - \rho_S(t)\tan(\beta_{\mathrm{LIM}}) \tag{5}$$

The elevation limit function is defined as

$$f_{\phi_{\mathrm{LIM}}}(t) = \left(\cos^{-1}\left\{\frac{\cos[\phi(t)]}{R(t)}\right\} - \phi(t)\right) - \left\{\cos^{-1}\left[\frac{\cos(\phi_{\mathrm{LIM}})}{R(t)}\right] - \phi_{\mathrm{LIM}}\right\} \tag{6}$$

and approximates the difference between true elevation and the elevation limit for site/satellite geodetic angles. The range limit function is

$$f_{\mathrm{RANGE}}(t) = R(t) - R_{\mathrm{LIM}} \tag{7}$$

Any time one of these functions equals zero, the time of crossing is determined from the polynomial root; a quadrant check for azimuth limits is also necessary to test root validity. The limit functions are designed to reduce polynomial wiggle, thereby increasing the accuracy of the curve fit. An advantage of this fitting process is the localized curve model, where the curve must be continuous but need not conform to a sinusoidal-like function.

Curve Fitting

There are many techniques available to accomplish curve fitting. To alleviate the problems associated with restrictive sinusoidal fits or high-order generalized polynomials, a numerical technique called quartic blending is developed. This method is an extension of the work done in Ref. 4.

A series of polynomial functions, each defined by five data points, is used to approximate a waveform. Curve fitting by quartic blending uses six consecutive points to create two fourth-order curve functions. The first curve is created from the first five data points with the second curve created from data points two through six. As shown in Fig. 1, the curve segments passing through the central points are blended into a single fifth-order polynomial. The equation to accomplish the blending is chosen to match the first quartic's slope and its derivative at the third point and match the second quartic's slope and its derivative at the fourth point. This blending process is repeated until the data set is exhausted, resulting in a second-order continuous curve created from numerous localized quintic polynomials.

A quartic polynomial $F(\tau)$ passing through five consecutive points $(p_0, p_1, p_2, p_3, p_4)$ on a uniform interval that corresponds to the index is defined as

$$F(\tau) = \gamma_1\tau^4 + \gamma_2\tau^3 + \gamma_3\tau^2 + \gamma_4\tau + \gamma_5 \qquad (0 \le \tau \le 4) \tag{8}$$

where

$$\gamma_5 = p_0 \tag{9a}$$

$$\gamma_4 = (-50p_0 + 96p_1 - 72p_2 + 32p_3 - 6p_4)/24 \tag{9b}$$

$$\gamma_3 = (35p_0 - 104p_1 + 114p_2 - 56p_3 + 11p_4)/24 \tag{9c}$$

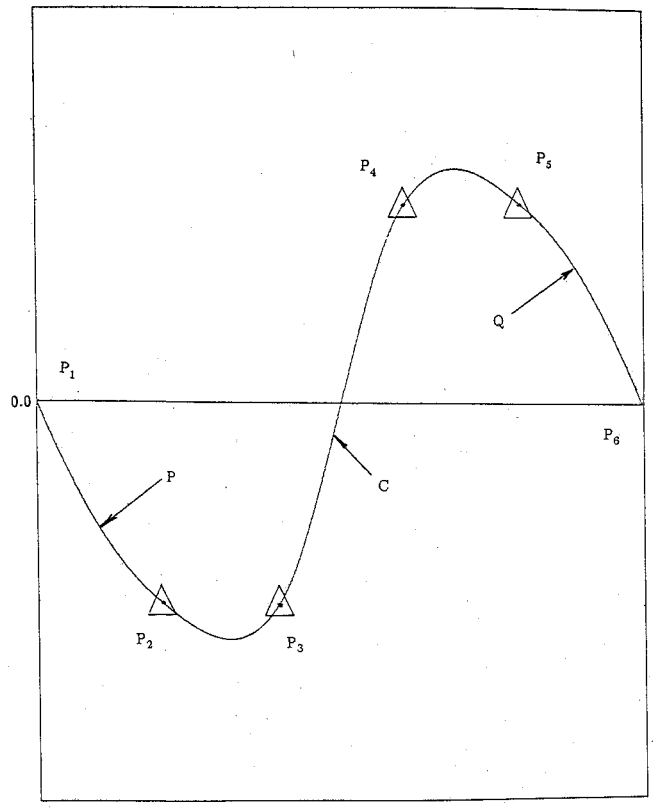

Fig. 1 Nomenclature for quartic blending.

$$\gamma_2 = (-10p_0 + 36p_1 - 48p_2 + 28p_3 - 6p_4)/24 \quad (9d)$$

$$\gamma_1 = (p_0 - 4p_1 + 6p_2 - 4p_3 + p_4)/24 \quad (9e)$$

The point, slope, and its derivative with respect to τ at midpoint are

$$F(\tau)\Big|_{\tau=2} = F(2) = 16\gamma_1 + 8\gamma_2 + 4\gamma_3 + 2\gamma_4 + \gamma_5 \quad (10)$$

$$\frac{dF(\tau)}{d\tau}\Big|_{\tau=2} = \dot{F}(2) = 32\gamma_1 + 12\gamma_2 + 4\gamma_3 + \gamma_4 \quad (11)$$

$$\frac{d^2F(\tau)}{d\tau^2}\Big|_{\tau=2} = \ddot{F}(2) = 48\gamma_1 + 12\gamma_2 + 2\gamma_3 \quad (12)$$

Quartic blending is accomplished by using six consecutive points (P_1, P_2, P_3, P_4, P_5, P_6), as shown in Fig. 1. The first quartic P ranges from P_1 to P_5, whereas the second quartic Q ranges from P_2 to P_6. The quintic C curve, ranging between P_3 and P_4, combines the two quartics so as to match the P curve to second order at P_3 and match the Q curve to second order at P_4. This is done by using Eqs. (8–12) to determine P, $\dot{P}$, and $\ddot{P}$ at P_3 and also to determine Q, $\dot{Q}$, and $\ddot{Q}$ at P_4. After some algebraic manipulation, the equation for $C(T)$ becomes

$$C(T) = \alpha_1 T^5 + \alpha_2 T^4 + \alpha_3 T^3 + \alpha_4 T^2 + \alpha_5 T + \alpha_6 \quad (0 \le T < 1) \quad (13)$$

where

$$\alpha_6 = P_3 \quad (14a)$$

$$\alpha_5 = (2P_1 - 16P_2 + 16P_4 - 2P_5)/24 \quad (14b)$$

$$\alpha_4 = (-P_1 + 16P_2 - 30P_3 + 16P_4 - P_5)/24 \quad (14c)$$

$$\alpha_3 = (-9P_1 + 39P_2 - 70P_3 + 66P_4 - 33P_5 + 7P_6)/24 \quad (14d)$$

$$\alpha_2 = (13P_1 - 64P_2 + 126P_3 - 124P_4 + 61P_5 - 12P_6)/24 \quad (14e)$$

$$\alpha_1 = (-5P_1 + 25P_2 - 50P_3 + 50P_4 - 25P_5 + 5P_6)/24 \quad (14f)$$

In-view and out-of-view times occur whenever a quintic limit function changes sign; that is, whenever $C(T)$ equals zero. The roots of $C(T)$ are ignored if they are imaginary, repeating, or outside the range of T. Any remaining roots designate the *unitized* in-view and out-of-view times between points P_3 and P_4. Because the roots of interest are in the interval (0, 1), a quick test determines if further processing is necessary; if $\alpha_6 > 0$ and

$$\text{MIN}(\alpha_5,\ \alpha_5+\alpha_4,\ \alpha_5+\alpha_4+\alpha_3,\ \alpha_5+\alpha_4+\alpha_3+\alpha_2,\ \alpha_5+\alpha_4+\alpha_3+\alpha_2+\alpha_1) > -\alpha_6$$

or if $\alpha_6 < 0$ and

$$\text{MAX}(\alpha_5,\ \alpha_5+\alpha_4,\ \alpha_5+\alpha_4+\alpha_3,\ \alpha_5+\alpha_4+\alpha_3+\alpha_2,\ \alpha_5+\alpha_4+\alpha_3+\alpha_2+\alpha_1) < -\alpha_6$$

then no root can exist in the interval.

A Newton-Raphson[6] method is used to determine if any real unique roots exist in the interval (0, 1). An excellent initial estimate is found by approximating the quintic polynomial on the interval as a quartic; Eqs. (8) and (9) are used for the points [$C(0)$, $C(0.25)$, $C(0.5)$, $C(0.75)$, $C(1)$] with the quartic solved in closed form.[7] If no unique real roots exist in the quartic interval, then it is assumed no such roots exist for the quintic interval. If a root does exist in the quartic interval (0, 4), it is divided by 4 to correspond to the quintic interval (0,1) and used to start the Newton-Raphson search. Once a single root is found, it is factored out, and the resulting quartic is solved in closed form.

By choosing six consecutive values of ρ_S, ρ_E, and ρ_Z from a reference file, the α coefficients for the limit functions are easily computed for $C(T)$, and the real unique root(s) T_{ROOT} found. If the root is within bounds, a different set of α coefficients α_t are computed using the times that correspond to the original chosen values. This resulting $C_t(T)$ equation yields the in-view or out-of-view time associated with T_{ROOT}. When a crossing time has occurred, quartic blending is used again to determine $\rho_S(T_{\text{ROOT}})$, $\rho_E(T_{\text{ROOT}})$, and $\rho_Z(T_{\text{ROOT}})$; those values are then used to produce azimuth, elevation, and range information from Eqs. (2–4).

Simulation

The visibility windows and associated antenna-pointing parameters obtained by this method are compared with those from a standard general perturbations step-by-step integration. For this study, the site and satellite are advanced in intervals of 1/10 s, and a visibility check is performed. These results, which serve as the *truth* for purposes of accuracy, are obtained by influencing a satellite by the following first-order secular rates caused by mass anomalies[8]:

$$\bar{n} = n_0\left[1 + \frac{3}{2}J_2\frac{\sqrt{1-e^2}}{p^2}\left(1 - \frac{3}{2}\sin^2 i\right)\right] \quad (15)$$

$$\dot{\Omega} = -\left(\frac{3}{2}\frac{J_2}{p^2}\cos i\right)\bar{n} \quad (16)$$

$$\dot{\omega} = \left[\frac{3}{2}\frac{J_2}{p^2}\left(2 - \frac{5}{2}\sin^2 i\right)\right]\bar{n} \quad (17)$$

For the Earth-fixed tracking station, the site is initialized at the principal axis and its future position given by[8]

$$x = G_1\cos(\phi_{\text{LAT}})\cos(\theta) \quad (18)$$

$$y = G_1\cos(\phi_{\text{LAT}})\sin(\theta) \quad (19)$$

$$z = G_2\sin(\phi_{\text{LAT}}) \quad (20)$$

$$G_1 = \frac{1}{\sqrt{1 - e_e^2\sin^2(\phi_{\text{LAT}})}} + H \quad (21)$$

$$G_2 = \frac{1 - e_e^2}{\sqrt{1 - e_e^2\sin^2(\phi_{\text{LAT}})}} + H \quad (22)$$

For quartic blending, the site and satellite are advanced in 3-min intervals, and the limit functions are checked for crossing times.

Classical orbital elements from the United States Space Command satellite catalog are used as test data for this study and are listed in Table 1. These elements were obtained by sorting the catalog, which includes 7000 satellites, by orbital eccentricity, mean motion, and inclination. The satellites with the least, average, and greatest values of eccentricity, mean

Table 1 Classical orbital elements[a]

Object	N, rev/solar day	e	i, deg
1	1.00272141	0.0000032	0.0956
2	8.36589235	0.0080158	90.0175
3	0.24891961	0.9363060	64.9874
4	0.21467209	0.0668128	57.3500
5	13.37659679	0.0145072	90.2619
6	16.09769232	0.0078742	82.8709
7	1.00271920	0.0003109	0.0099
8	12.41552416	0.0036498	74.0186
9	13.84150848	0.0048964	144.6414

[a] $\omega = \Omega = MA = 0$ deg.

Table 2 One-day site/satellite timetable for satellite 3

	In view	Out of view
Quartic blending	329.1	352.5
Truth simulation	329.9	352.6
Absolute difference	0.8	0.1

Table 3 One-day site/satellite timetable for satellite 5

	In view	Out of view
Quartic blending	354.7	648.1
	706.6	714.1
	41,430.9	41,689.1
	47,617.3	48,003.7
	84,436.3	84,650.8
Truth simulation	354.7	648.1
	706.7	714.2
	41,431.0	41,689.2
	47,617.4	48,003.8
	84,436.3	84,650.8
Absolute difference	0.0	0.0
	0.1	0.1
	0.1	0.1
	0.1	0.1
	0.0	0.0

Table 4 One-day site/satellite timetable for satellite 6

	In view	Out of view
Quartic blending	498.4	539.6
Truth simulation	497.4	539.6
Absolute difference	1.0	0.0

Table 5 One-day site/satellite timetable for satellite 8

	In view	Out of view
Quartic blending	356.2	644.7
	7,539.8	7,911.0
	37,783.3	37,855.8
	44,244.3	44,820.3
	83,997.9	84,052.9
Truth simulation	356.2	644.8
	7,539.9	7,911.0
	37,783.3	37,855.9
	44,244.5	44,820.3
	83,998.2	84,052.9
Absolute difference	0.0	0.1
	0.1	0.0
	0.0	0.1
	0.2	0.0
	0.3	0.0

motion, and inclination are used as test data. Also, for this study, the Earth-fixed tracking station is placed at the United States Air Force Academy and is initialized at the vernal equinox; the station coordinates are 104° west longitude, 39° geodetic latitude, with 2.9-km deviation above the ellipsoid.

Simulation Results

Tables 2–6 show the viewing times for a 1-day simulation using the parameters of Table 1. Timetables for objects 1, 2, 4, and 7 were not included because those objects were not visible to the restricted site. The method of quartic blending (with 3-min time steps) reduces computer processing time by 89% over a 5-s brute force approach. Also, the results of this method differ by less than 1 s when compared with a 0.1-s step truth model.

Table 6 One-day site/satellite timetable for satellite 9

	In view	Out of view
Quartic blending	52,035.4	52,284.1
	57,962.6	58,299.9
	63,878.0	64,219.2
	69,725.3	70,114.0
	75,511.5	75,981.5
Truth simulation	52,035.5	52,284.2
	57,962.7	58,300.0
	63,878.0	64,219.3
	69,725.3	70,114.1
	75,511.5	75,981.5
Absolute difference	0.1	0.1
	0.1	0.1
	0.0	0.1
	0.0	0.1
	0.0	0.0

Table 7 Maximum difference in timetable pointing parameters

Object	Azimuth, deg	Elevation, deg	Range, km
3	0.1	0.0	1.9
5	0.1	0.0	0.4
6	0.3	0.2	6.6
8	0.0	0.0	1.3
9	0.0	0.0	0.4

Table 7 shows the accuracy of azimuth, elevation, and range associated with the timetables. The antenna-pointing parameters are very accurate, with the largest differences occurring in range. The range inaccuracies, especially for a low-altitude satellite, are caused by rapidly varying data on an overhead pass; if greater accuracy is desired, smaller time steps should be taken to achieve a better curve fit. The extensive results, representing the extremes of the tracked satellite population, demonstrate that this method can be used to support operational missions.

Conclusions

This paper presents a very powerful method to rapidly compute an accurate site/satellite timetable with associated antenna-pointing parameters for an oblate Earth in the presence of site restrictions. The test results demonstrate the completeness of this routine, which is free of orbital restrictions. Because the ephemeris generation and visibility determination are distinct problems, this allows the user to tabulate $\rho_S(t)$, $\rho_E(t)$, and $\rho_Z(t)$ to any desired accuracy from existing orbit propagation methods. Thus, if one wishes to perform parametric studies using site/satellite communication links as the performance index, perhaps generating a J_2-based reference file will suffice. Also, for programs requiring precise knowledge about viewing times, the designer can generate $\rho_S(t)$, $\rho_E(t)$, and $\rho_Z(t)$ tables using Cowell's method. For platforms with rapidly varying trajectories, the user can generate a very dense data set to accomplish curve modeling, provided the motion does not become discontinuous, especially near viewing entrance or exit. This logic can also be integrated on board the satellite computer to support autonomous operations; the computer generates timetables for a target set and then activates various instruments and operating modes once a site comes into view.

This approach is not limited to constraints in azimuth, elevation, and range or to quartic blending of the defined functions. Other constraints, such as satellite illumination by the sun or satellite in view of a data relay satellite, can be incorporated in the logic using the visibility function of Ref. 4. Parabolic blending may be substituted for quartic blending to reduce complexity, but this causes accuracy to decrease for the same time step; if smaller steps are taken to regain accuracy, then processing time will increase.

References

[1]Escobal, P. R., "Rise and Set Time of a Satellite about an Oblate Planet," *AIAA Journal*, Vol. 1, No. 10, 1963, pp. 2306–2310.

[2]Lawton, J. A., "Numerical Method for Rapidly Determining Satellite-Satellite and Satellite-Ground Station In-View Periods," *Journal of Guidance, Control, and Dynamics*, Vol. 10, No. 1, 1987, pp. 32–36.

[3]Alfano, S., Negron, D., Jr., and Wright, D. D., "The Method of Ratios," *Journal of the Astronautical Sciences*, Vol. 40, No. 2, 1992, pp. 297–309.

[4]Alfano, S., Negron, D., Jr., and Moore, J. L., "Rapid Determination of Satellite Visibility Periods," *Journal of the Astronautical Sciences*, Vol. 40, No. 2, 1992, pp. 281–296.

[5]Bate, R.R., Mueller, D.D., and White, J.E., *Fundamentals of Astrodynamics*, Dover, 1971, pp. 83–98 and 387–390.

[6]Hildebrand, F. B., *Introduction to Numerical Analysis*, Dover, New York, 1987, pp. 575–578.

[7]Abromowitz, M., and Stegun, I. A., *Handbook of Mathematical Functions*, Applied Mathematics Series 55, National Bureau of Standards, Washington, DC, pp. 17–18.

[8]Escobal, P. R., *Methods of Orbit Determination*, Krieger Publishing Co., Malabar, FL, 1965, pp. 360–369.

Alfred L. Vampola
Associate Editor